Journal of Environmental Chemical Engineering 12 (2024) 112650

Contents lists available at ScienceDirect

Journal of Environmental Chemical Engineering

journal homepage: www.elsevier.com/locate/jece

Standardized methodology for performance evaluation in using polyaniline-based adsorbents to remove aqueous contaminants

Akbar Samadi [a], Lingxue Kong [a], Wenshan Guo [b], Mika Sillanpää [c,d,e], Inci Boztepe [a], Chengwen Song [f], Qingyi Zeng [g], Shuaifei Zhao [a,f,*]

[a] *Deakin University, Geelong, Institute for Frontier Materials, VIC 3216, Australia*
[b] *School of Civil and Environmental Engineering, University of Technology Sydney, Sydney, NWS 2007, Australia*
[c] *Functional Materials Group, Gulf University for Science and Technology, Mubarak Al-Abdullah, 32093 Kuwait, Kuwait*
[d] *School of Technology, Woxsen University, Hyderabad, Telangana, India*
[e] *Centre of Research Impact and Outcome, Chitkara University Institute of Engineering and Technology, Chitkara University, Rajpura-140401, Punjab, India*
[f] *College of Environmental Science and Engineering, Dalian Maritime University, Dalian 116026, PR China*
[g] *School of Resources & Environment and Safety Engineering, University of South China, Hengyang 421001, PR China*

ARTICLE INFO

Keywords:
Adsorption
Adsorption kinetics
Adsorption thermodynamics
Polyaniline adsorbent
Pollutant removal

ABSTRACT

In literature, mistakes and inconsistencies in evaluation of the adsorption equilibrium, kinetics, and thermodynamics in pollutants removal often exist. Here, we review these mistakes and propose a standardized methodology, with a focus on polyaniline (PANI)-based adsorbents to correctly determine the adsorption equilibrium data, kinetic rates, equilibrium time, and adsorption capacity. Removal of aqueous pollutants by PANI-based adsorbents through well-designed experiments predominantly involves monolayer chemisorption. The nature of adsorption, whether heterogeneous or homogeneous, is contingent upon the morphological characteristics and distribution of functional groups of the adsorbents. The literature reflects a multitude of complexities in the implementation of adsorption experiments and the subsequent analysis of results. Researchers have attempted to address these complexities, yet variations in findings remain due to the diverse experimental conditions applied. This study critically examines existing methodologies and their conditions to develop a distinctive approach for rational experimental design, meticulous sampling, and accurate calculations. Controversial descriptions regarding adsorption equilibrium, kinetics and thermodynamics are scrutinized and the scientifically reasonable methodologies are presented. Finally, the main steps in determining the adsorption mechanisms via physiochemical studies and adsorption experiments are recommended. This study contributes insightful perspectives to the field by offering a more robust and standardized methodology to conduct adsorption experiments and interpret adsorption results, thereby enhancing the reliability and comparability of findings in adsorption.

1. Introduction

The crucial significance of eliminating pollutants from water and air has catalyzed researchers to explore and create new technologies, such as adsorption, which is economical and simple [1–4]. Conventional adsorbents, including activated carbon, natural zeolites, alumina, biochar, and clay minerals, exhibit limited effectiveness [5]. Hence, there is a growing interest in the development of polymer nanocomposites. Polyaniline (PANI), a stable and conductive polymer with a ring structure and nitrogen-substituted derivatives, has been widely used for removing pollutants, especially heavy metals [6–8] and dyes [9,10]. Its popularity has surged owing to its potential for effectively removing pollutants from water [5,11,12]. PANI has several advantages, including easy purification, simple synthesis, tunable morphology, chemical regenerability, affordability of precursors, and the capability to blend seamlessly with other polymers [13–15]. The imine groups of PANI provide the primary adsorption sites for ions [16]. However, the adsorption performance of PANI can be compromised by its inherent limitations, such as low processing capacity, aggregation, rigidity, and poor solubility [17,18].

Abbreviations: DR, Dubinin-Radushkevich; FTIR, Fourier-transform infrared spectroscopy; GO, Graphene oxide; INPD, Intraparticle diffusion; PANI, Polyaniline; PFO, Pseudo-first-order; PSO, Pseudo-second-order; RP, Redlich-Peterson; XPS, X-ray photoelectron spectroscopy.

* Corresponding author at: Deakin University, Geelong, Institute for Frontier Materials, VIC 3216, Australia.

E-mail address: s.zhao@deakin.edu.au (S. Zhao).

https://doi.org/10.1016/j.jece.2024.112650
Received 4 February 2024; Received in revised form 27 March 2024; Accepted 28 March 2024

To address the aggregation problem of PANI and enhance its adsorption performance, various PANI nanocomposites have been developed [19,20]. Strategies such as copolymerization [21,22], use of PANI derivatives [21,23], and preparation of nanocomposites with polymers [24–26] have been commonly employed to improve the adsorption capacity of PANI. Various fillers, such as clays [27–29], magnetic materials [30,31], low-cost bio-wastes [32], and 2D materials [33] have been used to enhance the functionality, surface area, or magnetic properties of PANI. Fig. 1 provides an overview of the distinct features and key advantages associated with different fillers of PANI-based adsorbents. This study systematically investigates the mechanisms on the adsorption of pollutants onto PANI-based adsorbents through a thorough analysis of adsorption kinetics, isotherms, and thermodynamics.

Adsorption experiments play a pivotal role in elucidating the adsorption isotherms, kinetics, and thermodynamics of various pollutants [34,35]. The primary aim of these experiments is to ascertain the adsorption equilibrium data and kinetic rates of adsorption. The discussion in this context delves into the frequently reported adsorption isotherms for PANI-based adsorbents, emphasizing their types and relevance in determining equilibrium time and adsorption capacity. The Langmuir isotherm, in particular, holds significance for studying adsorption thermodynamics, offering a physically meaningful derivation from the analysis of the adsorption reaction [36]. Evaluation of adsorption equilibrium data is crucial for determining the capacity of specific pollutant-adsorbent pairs. However, achieving adsorption equilibrium capacity is not instantaneous, with mass transfer resistance impeding the adsorption rates [37]. Therefore, it becomes imperative to develop an experimental methodology that can accurately determine both adsorption equilibrium data and kinetic rates. This methodology entails selecting a suitable reactor type for the designated powdered or granular adsorbent, calibrating the optimal initial concentration and particle size of the adsorbent, establishing a sampling procedure for accurately determining the equilibrium time of adsorption rates, and providing adequate agitation to mitigate unnecessary diffusion resistance.

Theoretical analysis of isotherm models is routinely utilized to assess the nature of adsorption. However, discussions regarding the potential errors in experiments and data analysis of empirical equations for adsorption models have been prevalent, given their tendency to generate inaccurate conclusions [38–40]. Despite the theoretical connections of Langmuir and Freundlich isotherm models to the nature of adsorption, the accuracy in determining adsorption nature through experimental data is compromised due to various factors, such as errors in experiments and linearization methods. In addition, these isotherms are often empirical, lacking a fundamental connection to the underlying adsorption mechanism.

The pseudo-second-order (PSO) model has higher correlation coefficients than the pseudo-first-order (PFO) model, suggesting chemisorption as the rate-limiting step [41]. However, caution is warranted as this observation may introduce bias toward the PSO model, primarily resulting from the collection of more data near the equilibrium point [37,42]. While both PFO and PSO models are applied to a wide range of data, relying solely on them for determining the adsorption mechanism is not advisable. Non-linear regression methods, diffusion models, and the consideration of various variables, such as agitation, sorbent size, solute concentration, activation energy, adsorbent mass, and solution temperature have been applied to enhance the accuracy of the kinetic models and to elucidate the adsorption mechanism [43–45]. Furthermore, the intraparticle diffusion (INPD) model proves valuable in identifying the rate-controlling steps and difference between chemical and physical adsorption [46].

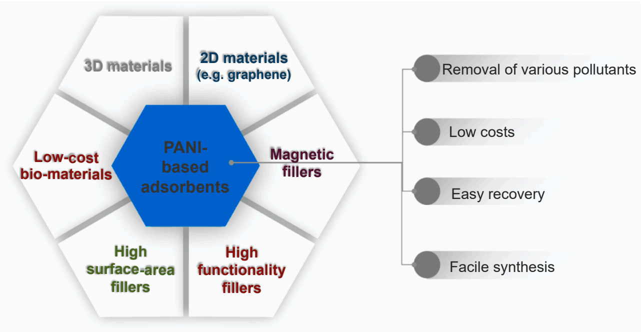

Fig. 1. Diverse types of PANI-based adsorbents with different fillers and their key advantages [5].

Using isotherm constants to calculate thermodynamic parameters in the van’t Hoff equation is a solid theoretical foundation, due to the absence of a direct correlation between isotherm and thermodynamic equilibrium constants [40]. The common practice of employing isotherm constants with dimensions and no inherent physical significance for determining thermodynamic parameters has introduced errors in their calculation and interpretation [47–49]. Derivation of the Langmuir isotherm model from reaction and equilibrium relations results in the dimensionless Langmuir adsorption coefficient [40,50,51], providing a theoretically verified approach to determine the equilibrium constant using the distribution or partition coefficient [52].

This paper discusses the mechanisms that govern the adsorption of pollutants onto PANI-based adsorbents through an analysis of adsorption kinetics, isotherms, and thermodynamics. Specifically, we demonstrate the incorporation of pertinent isotherms for calculating the adsorption heat and the adsorption mechanism. The Langmuir equation is utilized solely to determine the maximum (equilibrium) adsorption capacity and thermodynamic parameters. The discussion addresses potential errors in experiments and data analysis, offering significant insights into factors that can lead to inaccurate conclusions. Furthermore, methods for determining kinetic models and describing the adsorption mechanism are provided. Additionally, we scrutinize the use of isotherm constants to calculate thermodynamic parameters and discuss the problems with dimensionless equilibrium constants.

2. Design of adsorption experiments

Various options exist for batch or continuous reactors suitable for adsorption experiments. Agitated reactors, well-suited for powdered adsorbents, facilitate easy washing of adsorbents from the reactor due to the solution flow [49,53,54]. Batch adsorption setups are frequently utilized to determine the adsorption capacity and rate [55]. Powdered adsorbents possess a high surface area, which expedites the adsorption process and diminishes the adsorption equilibrium time, rendering batch experiments a favored option for adsorption studies. Conversely, fixed bed reactors are suitable setups for granular adsorbents, eliminating the need for a separation step and providing an advantage over batch vessels [56]. Consequently, the fundamentals of batch slurry vessels are further discussed as they are more commonly employed in adsorption studies. However, it is crucial to note that the selection of reactor type should be judiciously considered based on the adsorbent properties and experimental objectives.

In a batch adsorption setup, a finite quantity of adsorbent is brought into contact with a specific concentration of pollutants in a solution, and adsorption transpires with the assistance of agitation to surmount hydrodynamic transport resistance [57]. If the reactor is excessively large or a continuous flow of the polluted solution is sustained, the pollutant concentration remains constant over time. However, in most instances, in a finite-sized agitated reactor, the pollutant concentration in the aqueous solution varies with time but remains constant in the bulk solution. Various types of batch reactors, predicated on the mixing types, are depicted in Fig. 2 [58,59]. The bottle-point method, involving taking 8–10 samples, is employed to determine the adsorption data [60]. Equilibrium is reached when the adsorbate concentration in both the

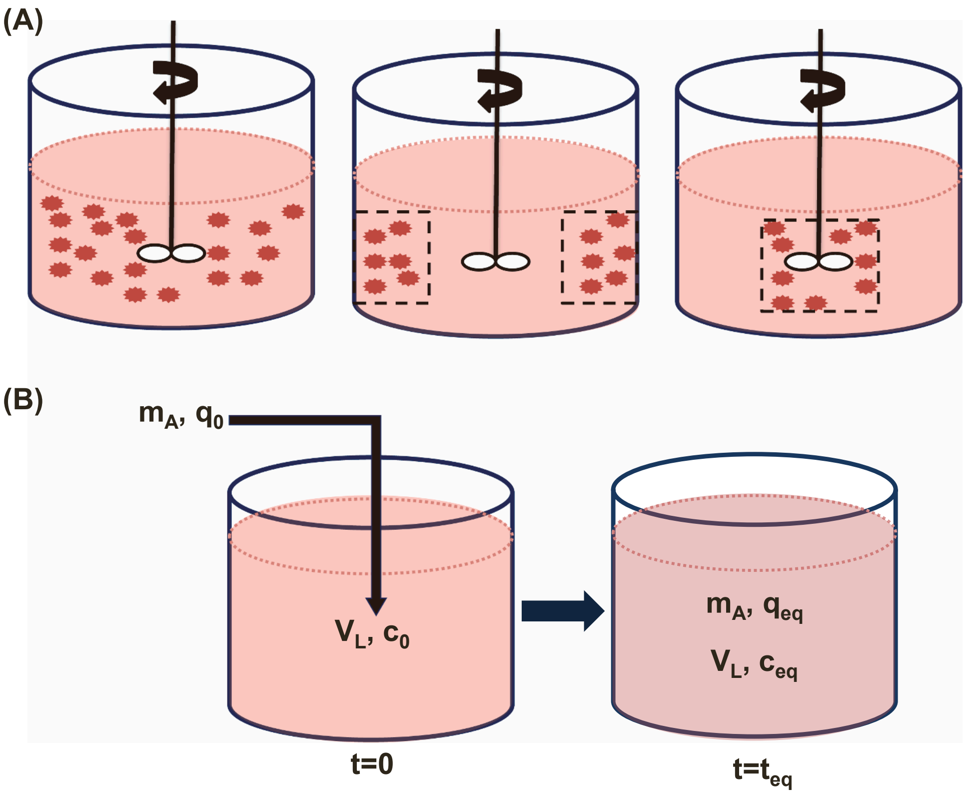

Fig. 2. Illustrations of (A) different types of batch reactors and (B) material flow of the batch adsorption system.

solution and on the adsorbent becomes constant. Precisely determining equilibrium time is crucial in adsorption studies, range from several hours to weeks, depending on several factors such as adsorbent properties, adsorbent-adsorbate interactions, and adsorption solution parameters [58,59]. The material balance and adsorption isotherm provide essential data of the adsorption process.

The pollutant removal efficiency is determined by the following equation:

$$Removal\% = \left(\frac{C_0 - C_e}{c_0}\right) \times 100 \tag{1}$$

where c_0 and c_e are the initial and equilibrium concentrations (mg·L^{-1}) of the pollutant in the solution, respectively.

The mass balance equation for adsorption on the particle surface is as follows [61,62]:

$$\rho_p D_s \nabla q + D_p \nabla c = \rho_p \partial q/\partial t \tag{2}$$

where ρ_p is the apparent density of the adsorbent, D_s is the surface diffusion coefficient, and D_p is the pore volume diffusion coefficient. The solution of this equation needs a relation for q versus c and the simplifications based on the predominant diffusion mechanism. The relationship between q and c can be described by the following equation:

$$q = q(c) \tag{3}$$

The mass diffusion on the particle surface (N_s) can be expressed by the following equation [61,62]:

$$N_s = k_f(c - c_s) = D_s \rho_p \partial q/\partial r + D_p \partial q/\partial r \tag{4}$$

And the total mass flux on the particle surface is given as follows:

$$N_s A_s = W_s \partial q_{av}/\partial t \tag{5}$$

where W_s is the adsorbent weight. q_{av} can be calculated by the following equation [56]:

$$q_{av} = \frac{\int_o^R (4\pi r^2 q) dr}{4\pi r^3/3} \tag{6}$$

The overall material balance after reaching the equilibrium leads to the calculation of equilibrium adsorption (q_e) [56]:

$$V_L(c_0 - c_{eq}) = m_A(q_{eq} - q_0) \tag{7}$$

$$q_{eq} = q_0 + \frac{V_L}{m_A}(c_0 - c_{eq}) \tag{8}$$

where c_0 and c_{eq} are the initial and equilibrium solution concentrations (unit e.g., kg/m^3), respectively, V is the volume of the solution (m^3), q_0 is the initial concentration of adsorbent, m_a is the weight of the adsorbent (kg) used. If q_0 is zero, then

$$q_{eq} = \frac{V_L}{m_A}(c_0 - c_{eq}) \tag{9}$$

For any bottle-point in the adsorption experiments, the adsorbed loading (q_t) at any time can be calculated by the same equation [56]:

$$q_t = \frac{V_L}{m_A} c_0 - \frac{V_L}{m_A} c_t \tag{10}$$

By using the slope of the operating line $\left(-\frac{V_L}{m_A}\right)$, different points on the isotherm curve can be determined by either varying the adsorbent dose while keeping c_0 constant (Fig. 3A) or varying c_0 while keeping the adsorbent dose constant (Fig. 3B) [56]. Since the accuracy of adsorption data is very important for the determination of equilibrium isotherms and kinetic parameters, it is recommended that:

(1) The sample selected for analysis should be representative of the adsorbent.

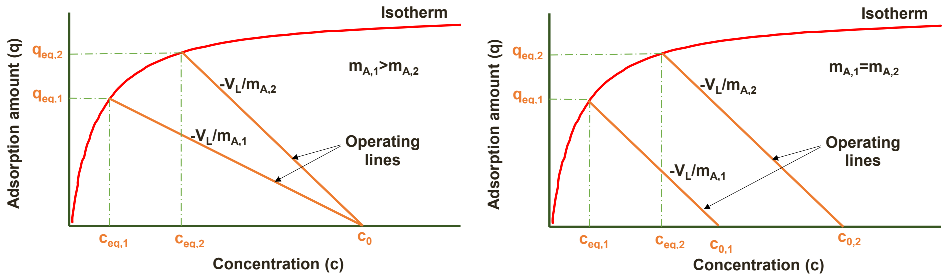

Fig. 3. The slope of the operating line $\left(-\frac{V_L}{m_A}\right)$, on the isotherm curve determined by (A) varying the adsorbent dose at constant c_0 and (B) varying c_0 at constant adsorbent dose.

(2) Prior to utilization, it is essential to conduct a series of preparatory procedures for the adsorbent, including thorough washing to remove impurities, subsequent drying to eliminate moisture content, and ultimately, storage in a desiccator to prevent reabsorption of water vapor.

(3) To avoid analytical errors, it is crucial to ensure that the weight difference of the adsorbent between the initial time and each subsequent measurement time is not excessively small.

(4) Given the significant heat of adsorption in aqueous phase adsorption, temperature control during adsorption tests is necessary.

(5) To make kinetic model data applicable to fixed bed systems, it is more expedient to calculate INPD coefficients by batch experiments and appropriate selection of kinetic model in cases of rapid mixing of solutions and powdered adsorbents. Designing adsorption batch experiments requires estimating the adsorption time, which is determined by factors such as particle size, mass transfer, and the ratio c_0/c_e. By ensuring sufficient stirring, external mass transfer resistance can be eliminated. Subsequently, the minimum adsorption equilibrium time (t_{min}) can be estimated using a pore diffusion model through the following equation [56]:

$$t_{\min} = \frac{T_{B,\min} \times r_p^2 \times \rho_P}{D_P \times c_0} \tag{11}$$

where r_p is the particle size, D_P is the pore diffusion coefficient, ρ_P is the particle density, and $T_{B,\min}$ is the minimum value for the dimensionless time which is defined as follows:

$$T_B = \frac{k_F \times a_{VR}}{\varepsilon_B \times D_B} t \tag{12}$$

where k_F is the film mass transfer coefficient, a_{VR} is the external surface area related to the reactor volume, $\varepsilon_B$is the bulk (bed) porosity, and D_B is the distribution parameter for the batch reactor. A rough estimate for $T_{B,\min}$ for surface diffusion and pore diffusion controlled mass transfer is 0.6 and 1, respectively, if only $c_{eq}/c_0<0.9$ [63]. However, the limitation of this equation is that the equilibrium loadings cannot be measured prior to conducting the isotherm experiments. As a result, the only feasible approach to estimating the equilibration time is to carry out kinetic tests prior to measuring equilibrium.

As to the kinetic experiments, a plot of c and q versus t is generated during the adsorption time, as shown in Fig. 4:

$$c = f_2(t) \tag{13}$$

where c is the concentration and t is the time. For any given point in the adsorption, the material balance can be expressed as follows:

$$q_t = \frac{V_L}{m_A}(c_0 - c_t) \tag{14}$$

Subsequently, the kinetic data is fitted to an appropriate kinetic model. In the case of adsorption in slurry reactor, it's notable that film diffusion only occurs during the initial stages of the adsorption process and can be safely neglected.

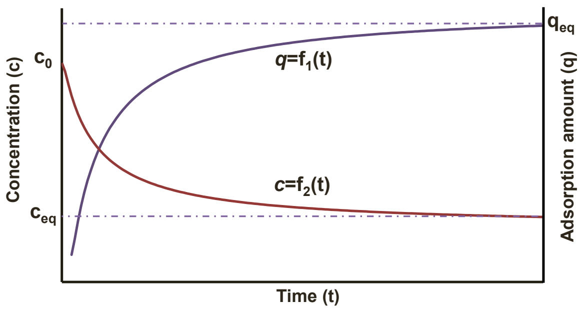

Fig. 4. The curves for c and q versus t plotted during the adsorption time in kinetic experiments.

3. Adsorption isotherms

The primary objective of studying adsorption isotherms is to correlate adsorption curves with isotherm models and determine the equilibrium time and capacity for a specific adsorbent-adsorbate pair. Isotherms are typically classified into five main categories, as depicted in Fig. 5 [64]. Type II is the most prevalent type for physical adsorption on relatively open surfaces, characterized by progressive adsorption from sub-monolayer to multilayer. A type III isotherm indicates weak interaction between the adsorbent and adsorbate, found in scenarios like water and alkanes on nonporous low-polarity solids like polytetrafluoroethylene. Type IV and V isotherms are associated with vapor adsorption by capillary condensation into small adsorbent pores. Briefly, for the adsorption of aqueous pollutants on PANI-based adsorbents, Type I (also known as Langmuir-type) adsorption provides the best prediction, with a monotonic approach to a limiting value that theoretically corresponds to the completion of a surface monolayer [7,65,66].

A variety of isotherm models is employe to interpret adsorption isotherm curves and investigate adsorption mechanisms [67]. For polyaniline-based adsorbents, various isotherm models such as Langmuir, Freundlich, Elovich, Temkin, Dubinin-Radushkevich (DR), Sips, and Redlich-Peterson (RP) models are commonly used to fit the adsorption data [30,48,68,69]. This section provides a comprehensive review of the most relevant isotherms for the adsorption of aqueous pollutants by PANI-based adsorbents. Additionally, some of these isotherm models, like Temkin and DR, are effectively employed to measure the adsorption energy and unveil the physicochemical nature of adsorption process [65,70].

Henry's isotherm model represents a linear equation describing the relationship between the equilibrium adsorbate concentrations present in both the liquid and adsorbed phases. It is particularly valuable for

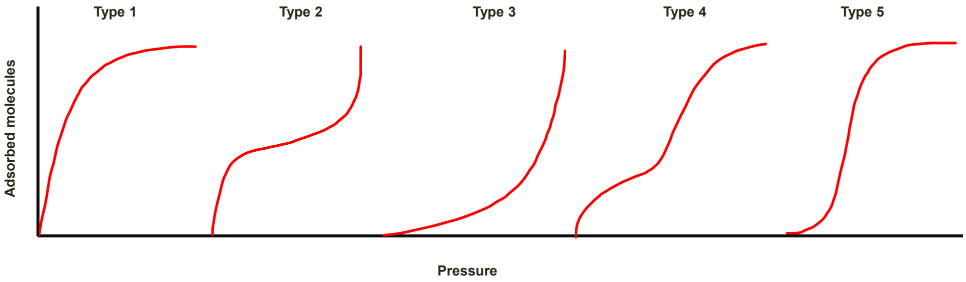

Fig. 5. The five types of adsorption isotherms according to the classification of Brunauer.

determining the initial slope of the adsorption curve at lower adsorbate concentrations [71]. In the interpretation of adsorption data, two-parameter models play a crucial role, offering convenient analysis due to their linearization properties and meaningful physical parameter interpretations. Notable examples of such models include the Hill-Deboer model, Fowler-Guggenheim model, Langmuir isotherm, Freundlich isotherm, DR isotherm, Temkin isotherm, Flory-Huggins isotherm, Hill isotherm, Halsey isotherm, Harkin-Jura isotherm, Jovanovic isotherm, Elovich isotherm, and Kiselev isotherm [72]. For the adsorption of aqueous pollutants by PANI-based adsorbents, this discussion focuses on four prominent two-parameter models, i.e., Langmuir, Freundlich, Temkin, and DR isotherms.

The Langmuir isotherm stands as a foundational model in theoretical adsorption investigations [73]. This model postulates a homogeneous surface with uniform energy, assuming a fixed number of adsorption sites for monolayer formation and reversible adsorption. The Langmuir isotherm equation can be expressed in a linear form as follows [73]:

$$\frac{1}{q_e} = \frac{1}{c_e b q_m} + \frac{1}{q_m} \tag{15}$$

The Langmuir isotherm equation relates the equilibrium adsorbate loading (q_e, mg·g^{-1}) to the equilibrium concentration of adsorbate (c_e, mg·L^{-1}) using two constants, namely the maximum adsorbate loading (q_m, mg·g^{-1}) and the Langmuir adsorption equilibrium constant (b, L·mg^{-1}), which represents the adsorption affinity. This model assumes that adsorption occurs on a homogenous surface with equivalent energy, maintaining a fixed number of monolayer adsorption sites and allowing reversible adsorption. However, the Langmuir isotherm overlooks adsorbate/adsorbate interactions, failing to consider these interactions and deviating from experimental data in cases of high b values and chemical adsorption. For instance, Khadir et al. prepared a low-cost non-toxic sisal/polypyrrole/polyaniline composite via an *in-situ* chemical oxidative polymerization technique and observed that the Langmuir was less fitted than Freundlich model due to the dominance of chemisorption [74]. In addition, Duhan et al. reported that the Langmuir model deviated for heterogeneous adsorption, specifically for the adsorption of methylene blue dye by phytic acid doped polyaniline nanofibers [9]. Despite these limitations, the Langmuir isotherm can make accurate predictions at low and high concentrations or pressures. One of the essential characteristics of this isotherm is its dimensionless separation factor, which is a measure of the adsorption favorability and is denoted by R_L [75]:

$$R_L = \frac{1}{1 + bc_0} \tag{16}$$

The R_L value indicates whether the adsorption process is favorable ($R_L < 1$), unfavorable ($R_L > 1$), or irreversible ($R_L = 1$). The R_L value is determined by the value of the Langmuir adsorption equilibrium constant, b (L m·g^{-1}), and the initial concentration of the adsorbate, c_0 (mg·g^{-1}). Specifically, when the R_L value is between 0 and 1, the Langmuir isotherm predicts favorable adsorption, while an R_L value greater than 1 indicates unfavorable adsorption. An R_L value of 1 suggests irreversible adsorption. Khadir et al. have reported a separation factor below 1, indicating favorable adsorption of reactive orange 5 by the low-cost sisal fibers/polypyrrole/polyaniline bio-sorbent [74]. The Langmuir adsorption equilibrium constant (b value) can also be used as a rough indicator to distinguish between chemisorption and physisorption. Considering that PANI-based adsorbents consist of porous materials with nano/micro-sized pores [5], the Langmuir model is often suitably employed for fitting of isotherm data [7,65,66]. One remarkable feature of the Langmuir adsorption isotherm is that its derivation from the study of the adsorption reaction with physical meaning, which enables for the determination of thermodynamic parameters by modifying the b value to become dimensionless [40,67].

The Freundlich isotherm is a widely used multisite adsorption model for rough surfaces. The linear form of the Freundlich isotherm model can be expressed by Eq. (17) [76]:

$$\log q_e = \log K_F + \frac{1}{n} \log c_e \tag{17}$$

where the adsorption capacity (K_F) and intensity (n) are key parameters. The heterogeneity factor, $1/n$, provides insight into the adsorption process. When $1/n$ values lie between 0 and 0.5, the adsorption is favorable, whereas values between 0.5 and 1 indicate some obstacle to adsorption. When $1/n$ is greater than 1, chemisorption is dominant, making adsorbate adsorption rather difficult. Although the Freundlich isotherm readily fits adsorption data, it lacks a Henry law limit and a saturation limit. Consequently, it is often necessary to use another isotherm, such as Langmuir, to predict the equilibrium adsorption capacity. The Freundlich isotherm is frequently used in conjunction with the Langmuir isotherm to predict the adsorption behavior of PANI-based adsorbents toward aqueous pollutants. In some cases, the Freundlich model offers better predictions, particularly for chemisorption on heterogeneous surfaces [74]. However, it is crucial to recognize that, despite theoretical connections of the Langmuir and Freundlich isotherms with the nature of adsorption (i.e., chemisorption or physisorption), experimental data cannot accurately determine the adsorption nature due to various factors such as errors in experiments and linearization. Furthermore, these isotherms are empirical equations and do not have any fundamental relationship with the adsorption mechanism.

The Temkin model, another frequently applied two-parameter isotherm for fitting PANI-based adsorbents adsorption data of PANI-based adsorbents, considers indirect adsorbate/adsorbate interactions. It assumes that the heat of adsorption decreases linearly as surface coverage increases [77]. It is important to note that the Temkin isotherm is applicable within an intermediate range of adsorbate concentrations. The linear form of the Temkin isotherm can be expressed as follows:

$$q_e = \frac{RT}{b_T} \ln A_T + \frac{RT}{b_T} \ln c_e \tag{18}$$

where A_T is equilibrium binding constant (g^{-1}) and b is the heat of adsorption energy (J mol^{-1}). One of the primary advantages of the Temkin isotherm is its ability to calculate the heat of adsorption, which is valuable tool for determining whether adsorption is physisorption or chemisorption [78]. The Temkin model assumes indirect interactions between adsorbate molecules and postulates a linear decrease in the heat of adsorption with increasing surface coverage [78]. While the Temkin isotherm is valuable, it may be not appropriate for complex systems. Nevertheless, it has been applied by many researchers to study the adsorption of aqueous pollutants on PANI-based adsorbents. However, these studies have sometimes resulted in low regression values. The primary motivation for incorporating the Temkin isotherm has been to calculate the heat of adsorption and understand the physicochemical nature of adsorption [70,79,80].

In contrast, the Temkin isotherm has been frequently used to remove dyes and heavy metals by PANI-based adsorbents [47,81], with some studies showing better fitting values than either the Freundlich isotherm [47,78,81] or the Langmuir isotherm [82]. It is worth noting that the activation energies for physisorption processes typically fall in the range 5–40 KJ·mol^{-1}, whereas chemisorption processes are characterized by higher activation energies (40–800 KJ·mol^{-1}) [83]. However, the Temkin isotherm shares limitations with the Freundlich isotherm, lacking both a Henry law limit and a saturation limit. As a result, it may be not adequate for predicting the equilibrium adsorption capacity, and an alternative isotherm, such as the Langmuir isotherm, should be considered.

The Dubinin-Radushkevich (DR) equation is an empirical model used to explain the adsorption of aqueous pollutants on PANI-based adsorbents as follows [69,81]:

$$lnq_m = \ln q_e \pm \beta E^2 \tag{19}$$

In this model, β represents the DR constant and E is the mean adsorption energy. The DR model, initially proposed by Dubinin to explain the adsorption of subcritical vapors onto micro-porous solids based on potential theory and micro-pore volume filling, remains a valuable tool in adsorption studies [10]. This empirical model is primarily employed to identify adsorption mechanism involving Gaussian energy distribution onto heterogeneous surfaces [84]. However, it is limited in its suitability for an intermediate range of adsorbate concentrations because of its unrealistic asymptotic behavior, and it does not conform to Henry's law at low pressure. Despite its limitations in describing the removal of aqueous pollutants by PANI-based adsorbents due to its poor R^2 value [49,69,81], the DR model provides valuable information on the heat of adsorption because the adsorption process is divided into physisorption and chemisorption based on the E value. For example, Khadir et al. reported a low R^2 value (below 0.8) for the adsorption of Reactive Orange 5 onto polypyrrole/PANI adsorbents but used the E value to determine the adsorption mechanism [74].

In conclusion, among the various two-parameter isotherms, the Langmuir equation is commonly utilized to determine the maximum (equilibrium) adsorption capacity and thermodynamic parameters. On the other hand, the Temkin and DR isotherms are generally employed to calculate the heat of adsorption, providing valuable insights into the adsorption mechanism.

Three-parameter models, including the RP, Sips, and Toth isotherms, are commonly used for the removal of aqueous pollutants by PANI-based adsorbents [44,85]. The RP isotherm, acting as a hybrid of the Langmuir and Freundlich isotherms, is characterized by a true Henry value at infinite dilution. The linear form of the RP isotherm equation is represented by Eq. (20), where A is the RP isotherm constant (L·g^{-1}) and β is an exponent ranging from 0 to 1.

$$\ln\frac{c_e}{q_e} = \beta \ln c_e - \ln A \tag{20}$$

Researchers have employed this isotherm to investigate the shift from the Langmuir model to the Freundlich model at different adsorbate concentrations [44,86]. For instance, Shabandokht et al. [86] and Tanzifi et al. [85] reported low regression coefficient of RP model for the adsorption of Cr(VI) and methyl orange by PANI-based adsorbents in comparison with Langmuir and Freundlich isotherm models, suggesting no shift in adsorption mechanism during the adsorption process. In contrast, Debnath et al. reported a shift from the Langmuir to Freundlich isotherm upon increasing the temperature from 25 to 35 and 45 °C, suggesting that the surface heterogeneity becomes more pronounced at higher temperatures, and the adsorption shifts toward the Freundlich model [44]. In another study, Zheng et al. found that the Cr(VI) adsorption by KF/PANI is well-described by the RP isotherm, whereas the Cr(VI) adsorption by PANI is better represented by the Freundlich isotherm [87]. They attributed this finding to the low adsorption capacity of KF compared to that of PANI nanofibers.

The Sips isotherm, a combination of the Langmuir and Freundlich isotherms, is particularly useful for predicting adsorption on heterogeneous surfaces [85,88]. This model overcomes the limitation associated with the Freundlich model, where increased adsorbate concentration leads to increased adsorption. The linear form of the Sips isotherm is given by Eq. (21) [85]:

$$\beta_s \ln c_e = -\ln\left(\frac{K_s}{q_e}\right) + \ln a_s \tag{21}$$

where K_s and a_s are Sips isotherm model constants (L g^{-1}) and β_s is Sips isotherm exponent. In a study on the adsorption of methyl blue by PANI, Mohamed et al. found that the Sips model provided the best fit among Langmuir, Freundlich and Sips models [89]. In other studies, the Sips equation had a higher regression coefficient than the Freundlich model, but a lower coefficient than the Langmuir model, suggesting that the monolayer homogeneous adsorption is dominant in the system [85,90]. Overall, the two-parameter and three-parameter isotherms discussed above are the most frequently used models to predict the equilibrium parameters of the adsorption of aqueous pollutants on PANI-based adsorbents that follow the type II isotherm curve.

4. Adsorption kinetics

Investigating the kinetics of adsorption holds paramount significance as it helps in determining the adsorption performance and understanding the underlying adsorption mechanisms [36,55]. Mathematical models, rooted in reaction models and diffusion, are instrumental in capturing these dynamics. The adsorption diffusion process comprises three steps as depicted in Fig. 6 [72]: (A) Film diffusion or diffusion across the liquid film; (B) INPD or diffusion in the liquid contained in the pores and walls; (C) Adsorption-desorption on the active adsorbent sites. The second step can be evaluated by the INPD model, which is used to identify the rate-controlling step and difference between chemical and

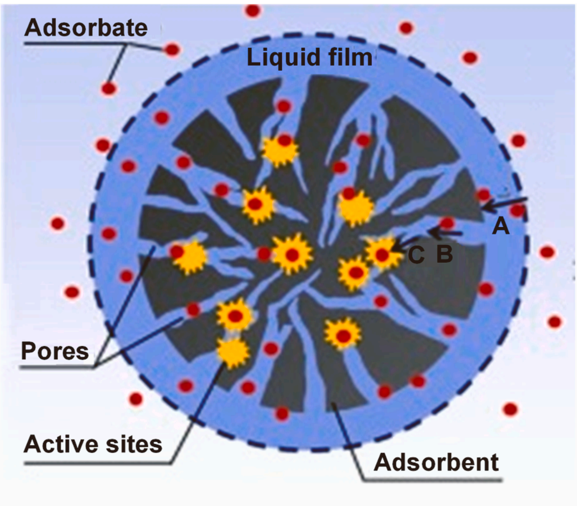

Fig. 6. Different steps of the adsorption [72].

physical adsorption [46]. Adsorption time, defined by Eq. (11) as an estimation, is the time required for the particle to penetrate from the liquid film and intraparticle diffusion path and then be adsorbed physically or chemically on the adsorbent surface. In chemical adsorption, the rate controlling step is mainly the INPD step, while the surface reaction and liquid film diffusion are rapid processes. However, as discussed above, sufficient stirring is required to eliminate external mass transfer resistance in the adsorption process.

Conversely, reaction models are derived from chemical reaction kinetics, treating adsorption as a single process without accounting for the sequential steps. It is important to highlight that while adsorption reaction models are frequently employed in the context of removing aqueous pollutants using PANI-based adsorbents, they do not take into account the physicochemical nature of the adsorption process [65,81,91]. Unfortunately, many publications have applied reaction kinetic models, attributing physical adsorption, which contradicts the basic principles of such models [86,91,92]. This issue is further compounded by inaccuracies in calculating the adsorption enthalpy, as discussed in the section on adsorption thermodynamics. Moreover, the Lagergren model is primarily a data modeling tool, and its physicochemical interpretation is erroneous. Hence, it is imperative to discuss the applicable adsorption kinetic models and their boundary conditions to properly incorporate them for the removal of dyes, heavy metals and emerging pollutants from water and wastewater using PANI-based adsorbents. The Lagergren kinetic model [93], also known as the PFO model, represents the earliest equation used to describe the adsorption rate based on the adsorption capacity. Its linear form is given by Eq. (22), where K represents the rate constant in units of minutes to the power of negative one.

$$\ln(q_e - q_t) = \ln q_e - Kt \tag{22}$$

The PFO model has often been employed alongside the PSO model, which considers the effect of adsorbent concentration or available active sites. Eq. (23) represents the linear form of the PSO model, where K_2 ($g{\cdot}mg^{-1}{\cdot}min^{-1}$) is the PSO rate constant.

$$\frac{t}{q_t} = \frac{1}{K_2 q_e^2} + \frac{t}{q_e} \tag{23}$$

The fundamental distinction between these two models lies in the consideration of adsorbent concentration or active sites. The PFO model overlooks these factors, making it well-suited for fitting data collected at short times or during the initial phases of adsorption experiments. On the other hand, the PSO model tends to be influenced by the abundance of data points near or at equilibrium time [42]. As a result, while both PFO and PSO models have found application in studies on the adsorption of aqueous pollutants by PANI-based adsorbents, only a few studies have reported superior fitting using PFO models. [79,94]. For instance, Kumar et al. performed adsorption of Cu(II) and Cr(VI) decontamination from wastewater using a recyclable multifunctional graphene oxide (GO)/SiO_2@PANI microspheres composite and reported similar regression coefficient values for PFO and PSO models [79]. However, they indicated that the PFO model offers a more accurate prediction of equilibrium adsorption capacity better than the PSO model. El-Sharkaway et al. conducted adsorption of methylene blue from aqueous solutions using PANI/GO or PANI/reduced GO composites [94]. They found that the PFO regression coefficient was significantly higher than that of the PSO model, implying a single species is considered on a heterogeneous surface. This means that the concentration of active sites on the surface of the adsorbent is much higher than the MB concentration, and only the MB dye concentration is significantly effective on the adsorption rate. Consequently, the adsorption reaction behaves more like a PFO reaction.

The precision of kinetic models in analyzing adsorption data is substantially influenced by experimental conditions. Specifically, the PFO model exhibits enhanced performance under conditions where the initial adsorbate concentration is low and data collection occurs over a short duration. This is attributed to the abundance of active sites on the adsorbent. The PFO model is particularly well-suited for scenarios where the adsorption process is rapid, and equilibrium is reached within a brief period, typically 20–30 minutes [62]. On the other hand, the PSO model has demonstrated efficacy in a diverse range of adsorption studies involving various pollutants, such as metal ions [95–97], dyes [98,99], and emerging pollutants [100–102], adsorbed by PANI-based adsorbents from aqueous solutions. These studies indicate that chemical adsorption occurs between functional groups of the aniline and ionic or polar groups of the adsorbates. In well-designed adsorption systems that represent real-world scenarios, both the adsorbent and adsorbate concentrations have significant influence on the adsorption rates.

Azizian has demonstrated that both PFO and PSO models can be derived from a single equation for the rate of adsorption given by Eq. (24) [36]:

$$\frac{d\theta}{dt} = k_a(C_0 - \beta\theta)(1-\theta) - k_d\theta \tag{24}$$

where θ is the coverage fraction $(0 < \theta < 1)$, C represents the initial molar concentration of solute, and k_a and k_d are the adsorption and desorption rate constants. The PFO model is obtained when the initial solute concentration is much higher than $\beta\theta$. An interesting finding of their work is that the adsorption coefficient of the PFO model (K) is a combination of the adsorption and desorption rate constants, as demonstrated by Eq. (25):

$$K = k_a C_0 + k_d \tag{25}$$

The procedure for obtaining the rate constants from the PFO model involves constructing a linear plot of K versus C_0, where the slope and intercept correspond to k_a and k_d, respectively and K is the equilibrium constant ($K = k_a/k_d$). However, if the initial solute concentration is not significantly high, the PSO model can be obtained by integrating the rate equation. At infinite time values, the Langmuir isotherm is achieved [36]. These observations suggest a shared origin for the PFO and PSO models, with their preference for fitting depends on experimental conditions rather than inherent physical considerations. To select the appropriate adsorption model, it is recommended to divide the adsorption experiments into two time-intervals and fit the PFO and PSO model for the 1st and 2nd part of the interval, respectively, and calculate the equilibrium adsorption capacity. Hence, due to the heterogeneity of solid surfaces, the application of PFO or PSO models in practical adsorption systems may not be suitable, as the effects of mass transport and chemical reactions cannot be distinguished [103].

Ho et al. conducted a comprehensive examination of the PFO and PSO models, reanalyzing data from previously published papers. They found that the correlation coefficients for the PSO model were greater than 0.996 for all systems at contact times of 120 minutes, suggesting that the previously reported PFO systems were better fitted with the PSO model. This conclusion was based on the assumption that the rate-limiting step may be chemisorption, involving valency forces through the sharing or exchange of electrons between the adsorbent and the adsorbate [41]. While there are comments on the Ho’s findings, it is essential to emphasize that both PFO and PSO models can be applied to most reported data, and it is not recommended to solely rely on kinetic or equilibrium models to determine the adsorption mechanism.

In conclusion, the prevailing trend in adsorption studies leans towards favoring the PSO model over the PFO model, because of the PSO model’s capacity to incorporate values close to the equilibrium state and address the complexities associated with the adsorbent surface [37]. However, relying solely on the PSO model for determining chemisorption is deemed meaningless. Instead, a comprehensive approach involving non-linear regression methods, diffusion models, and the evaluation of variable such as agitation speed, sorbent diameter, solute concentration, determination of activation energy, adsorbent mass and solution temperature, is recommended for a more accurate depiction of the adsorption mechanism. To gain deeper insight into the sorbate-sorbent interactions, physicochemical studies on the adsorbent surface are essential. It is emphasized that enthalpy alone is not a sufficient factor, and challenges arise regarding the reliability of equilibrium constants when calculating adsorption heat from van't Hoff equation, a topic to be further discussed in the "thermodynamics" section.

As mentioned previously, identifying the rate-controlling steps in the adsorption process is a key aspect of adsorption research. In solid-liquid adsorption, the mass transfer rate is controlled by external mass transfer and INPD [72]. Physical adsorption is primarily controlled by diffusion, while chemisorption is mainly rate-controlled by reaction kinetics in an appropriately designed experimental setup [44]. Optimal conditions, including an appropriate concentration of adsorbate, sufficient adsorbent weight, rapid mixing, fine particle size of the adsorbent, and judicious adsorbent selection, are expected to render INPD as the sole determinant of the rate. However, in certain scenarios, other diffusion resistance steps may also be significant. Furthermore, the decrease in the adsorbate concentration and active adsorbent sites in the final steps of adsorption, approaching the equilibrium time, can potentially alter the rate-controlling step [104]. Hence, the precise determination of the rate-controlling step in adsorption holds paramount importance. This knowledge, coupled with other investigative techniques, can be leveraged to scrutinize the adsorption mechanism and design an efficient adsorption process [105]. Weber and Morris introduced the **INPD model** as a means to better understand the rate-controlling step as follows [46]:

$$q_t = K_{id} t^{0.5} + C \tag{26}$$

where K_{id} represents the rate constant. The K_{id} value can be obtained by plotting q_t against $t^{0.5}$ However, in certain cases multi-linearity may be observed, indicating the presence of additional rate-controlling steps. The term "*C*" is suggested to be directly proportional to the boundary layer thickness. Initially, a sharp slope may be observed due to external diffusion, followed by INPD, and eventually, nearing to equilibrium state, the INPD slows down owing to the extremely low solute concentration in the solution [104,106]. The INPD model has been extensively employed to investigate the adsorption kinesics of the aqueous pollutants using PANI-based adsorbents [66,107]. However, the accurate application of this equation requires a meticulous division of the adsorption data into two or three time-intervals, with fitting performed separately for each interval [91,104,106]. Failure to adhere to this approach may result in poor line fitting and low regression coefficients [48]. Furthermore, multi-linear fitting regression is meaningless as the intervals are set manually [91,104]. The INPD model can also assist in selecting between PFO and PSO models. If INPD is identified the rate-controlling step, rather than the chemical reaction, then the concentration of the adsorbent is in excess and PFO model, or a series of PFO models, may be observed.

An alternative method to investigate the chemisorption on highly heterogeneous adsorbents is to employ the Elovich model, which describes the chemisorption of an adsorbate on a solid surface without the desorption of products. The model predicts that the adsorption rate decreases with time due to an increased surface coverage and is expressed in simplified linear form as follows [108]:

$$q_t = \frac{1}{\beta}\ln(\propto\beta) + \frac{1}{\beta}\ln(t) \tag{27}$$

where α is the initial adsorption rate constant (mg·g^{-1}·min^{-1}) and β is the Elovich adsorption constant related to the extent of surface coverage and activation energy for chemical adsorption in the Elovich model (g·mg^{-1}). Although the Elovich model does not provide a particular mechanism insight, it evaluates the surface heterogeneity of the adsorbents [74]. This model has been applied for the removal of aqueous pollutants by PANI-based adsorbents, and the reported regression coefficients (0.85–0.95) were lower than those obtained using the PSO and PFO models [74,80,109].

Overall, the adsorption of aqueous pollutants by PANI-based adsorbents predominantly involves a chemisorption process, characterized by a monolayer reaction facilitated by the abundance of nitrogen-rich functional amine and imine groups. Depending on the distribution and morphology of the functional groups, the system may be heterogeneous or homogeneous. Although the porous structure of the polymeric adsorbent allows for physisorption to take place, it is not the primary mechanism of adsorption. Diffusion may also be a rate-controlling step under inadequate agitation in the adsorption reactor, or as the adsorbate concentration decreases towards the end of the process. The INPD model proves useful in identify the contribution of the diffusion by analyzing different linear steps of the process. Additionally, when either the concentration of the adsorbent or the adsorbate is in excess, the PFO model may be observed.

5. Adsorption thermodynamics

To understand the nature and mechanism of adsorption and to examine the feasibility and thermal variation of the adsorption process, it is essential to determine the changes in system entropy and enthalpy [110]. The van't Hoff equation enables the calculation of three thermodynamic parameters: standard Gibbs free energy change, enthalpy change, and entropy change [111]. The equation is as follows:

$$\frac{d}{dT}\ln K_{eq} = \frac{\Delta H^0}{RT^2} \tag{28}$$

where *R* represents the universal gas constant (8.3144 J·mol^{-1}·K^{-1}) and *T* is the absolute temperature measured in Kelvin. The definition of Gibbs free energy and the Gibbs free energy equilibrium equation are combined as follows:

$$\Delta G^0 = \Delta H^O - T\Delta S^0 \tag{29}$$

and the Gibbs free energy equilibrium equation:

$$\Delta G^0 = -RT\ln K_{eq} \tag{30}$$

Thus, the following equation is derived:

$$\ln K_{eq} = -\frac{\Delta H^0}{R}\frac{1}{T} + \frac{\Delta S^0}{R} \tag{31}$$

The $\ln K_{eq}$ versus $1/T$ plot is commonly used to determine the heat of adsorption enthalpy (ΔH°, KJ·mol^{-1}) and entropy (ΔS°, KJ·mol^{-1}). A negative ΔH° and a positive ΔS° indicate an exothermic reaction that leads to increased randomness within the system, contributing to a favorable spontaneous reaction with a negative Gibbs free energy. However, the main challenge here is to accurately determine the thermodynamic equilibrium constant K_{eq} [40]. In the literature, the isotherm models are widely used to derive thermodynamic parameters for adsorption using the van't Hoff equation. This equation reveals a relationship between adsorption data and thermodynamic parameters. Despite its usefulness, inaccuracies and debates surround the correct application of this equation, as discussed by various authors [39,112,113]. The primary issue lies in the definite dimension of adsorption constants derived from isotherms, such as L·mmol^{-1} for the Langmuir sorption constant, rendering logarithmic computation invalid. Moreover, parameters in transcendental functions, such as logarithmic, exponential, and trigonometric functions, must be dimensionless. Unfortunately, K_{eq} in the van't Hoff equation has no dimension, and *K*-values with dimensions is mathematically incorrect and meaningless, leading to arbitrary values for ΔG and ΔS. To resolve this issue, the following equation is suggested [40,50,114]:

$$K_{eq} = \frac{1000 \times K_g \times MW_{ads} \times [adsorbate]^\circ}{\gamma} \tag{32}$$

where K_{eq} is the dimensionless thermodynamic equilibrium constant, MW_{ads} is molecular weight of adsorbate, K_g is the equilibrium constant of the best fitted isotherm model, such as K_L, the Langmuir equilibrium constant that are given in $\text{L}\cdot\text{mg}^{-1}$, γ is the coefficient of activity (dimensionless), and $[\text{Adsorbate}]^{\circ}$ is the standard concentration of the adsorbate (1 M). Regarding the physical meaning of Langmuir isotherm, derived by Azizian [36], it is recommended as the preferred model for this equation. The calculation assumes that the adsorbate solution is sufficiently diluted, allowing the activity coefficient to be treated as unity. It is crucial to adhere the principles of the chemical equilibrium when establishing the adsorption equilibrium, with the relationship between the reaction equilibrium constant and the isotherm constant extensively discussed in the literature [40,112,114]. For example, there is no theoretical connection between the constant in the empirical Freundlich isotherm and the thermodynamic equilibrium constant [112]. Therefore, attempts to make this constant dimensionless, such as the work done by Tarn et al. [114], are deemed meaningless. To clarify this further, when both Langmuir and Freundlich isotherms are fitted for adsorption, the calculation of thermodynamic parameters using both isotherm constants yields different values, highlighting the lack of a genuine relationship between isotherm constants and the equilibrium constant. However, researchers have endeavored to establish a connection between them, and the Langmuir isotherm is particularly valuable due to its potential for a theoretical relationship between isotherm constants and the equilibrium constant [40,114].

Lima et al. conducted a study to recalculate the thermodynamic parameters of published papers by correcting the equilibrium constant using this equation. The results demonstrated significant differences from the reported values [40]. Despite the widespread use of isotherm constants with dimensions and no physical meaning to determine thermodynamic parameters, the interpretation of many published thermodynamic investigations lacks significance [49,80,115]. Some authors attempted to use the partition coefficient $K_P = a_s/a_e$, where a_s is the activity of the adsorbate adsorbed onto the adsorbent, and a_e is the activity of the adsorbate in equilibrium solution. However, a few researchers incorrectly reported $C_e/(1-C_e)$ and C_{ad}/C_{eq} as a dimensionless equilibrium constant without providing any explanation or reference [109]. In contrast, the well-established and theoretically verified approach to determine the equilibrium constant was introduced by Biggar et al. using the distribution coefficient or partition coefficient in the following equation for adsorption equilibrium state [52]:

$$K_{eq} = \frac{a_s}{a_e} = \frac{\gamma_s}{\gamma_e}\frac{C_s}{C_e} \tag{33}$$

where a_s is activity of the adsorbed solute, a_e is activity of the solute in the equilibrium solution, c_s is the micrograms (μg) of solute adsorbed per milliliter of solvent in contact with the adsorbent surface, c_e is the μg of solute per milliliter of solvent in the equilibrium solution, and γ_s is the activity coefficient of the adsorbed solute, and γ_e is the activity coefficient of the solute in the equilibrium solution [52]. This equation of provides a dimensionless value for K_{eq}, although c_s is unknown and calculated using the following equation [116]:

$$c_s = \frac{(\rho_1/M_1)A_1}{\frac{s}{N(x/m)}} \tag{34}$$

where ρ_1 is the density of solvent ($\text{g}\cdot\text{mL}^{-1}$), M_1 is molecular weights ($\text{g}\cdot\text{mol}^{-1}$) of the solvent, A_1 is the cross-sectional area ($\text{cm}^2\cdot\text{mol}^{-1}$) of the solvent molecule, N is Avogadro’s number, j is the surface area of the adsorbent ($\text{cm}^2\cdot\text{g}^{-1}$), and x/m is specific adsorption ($\mu\text{g}\cdot\text{g}^{-1}$). At dilute solutions, γ_s/γ_e becomes unity, and hence:

$$K_{eq} = \frac{a_s}{a_e} = \frac{c_s}{c_e} \tag{35}$$

The values of K_{eq} can be obtained by plotting $\ln(c_s/c_e)$ versus c_s and extrapolating to zero c_s. Then, the standard free energy ΔG^0 (i.e., Eq. (30)), standard enthalpy ΔH^0, and the standard entropy ΔS^0 can be obtained:

$$\frac{\ln(K_{eq2})}{\ln(K_{eq1})} = -\frac{\Delta H^0}{R}\left(\frac{1}{T_2} - \frac{1}{T_1}\right) \tag{36}$$

$$\Delta S^0 = \left(\Delta H^0 - \Delta G^0\right)/T \tag{37}$$

Ahmad conducted a study on the thermodynamic parameters of a PANI/ZnO nanocomposite for the removal of Cr(VI) from aqueous solution using the Biggar equation. The results of the study indicated that the adsorption process was endothermic, spontaneous and accompanied by an increase in entropy [109].

In conclusion, the utilization of isotherm constants for calculating thermodynamic parameters in the van’t Hoff equation lacks substantial support due to the absence of a well-established theoretical correlation between isotherm and thermodynamic equilibrium constants. Nevertheless, some commendable endeavors have been made to establish the Langmuir isotherm model from reaction and equilibrium relations, resulting the dimensionless Langmuir adsorption coefficient [39,51,113]. Additionally, the dimensionless distribution coefficient (c_s/c_e) introduced by Biggar may be cautiously employed in the van’t Hoff equation to determine the thermodynamic parameters.

6. Adsorption mechanisms

To investigate the adsorption process, accurate determination of the adsorption mechanism is essential, and various tasks are involved, as briefly illustrated in Fig. 7. Firstly, an in-depth understanding of the chemistry of the adsorbent and adsorbate is required, including their functional groups, electric charge, hydrophobicity, and solubility, to evaluate the possible physicochemical reactions. Secondly, the morphology and surface area of each component should be analyzed using instrumental methods such as scanning electron microscope, Brunauer-Emmett-Teller analysis, X-ray powder diffraction, transmission electron microscopy, energy dispersive X-ray, and zeta potential analysis. These techniques can provide insights into the role of diffusion in the adsorption process.

X-ray photoelectron spectroscopy (XPS) is a powerful instrument utilizing AlK_{α} rays to provide information on elements located just a few tens of nanometers below the sample surface [117]. It can identify changes in bond energy, or chemical shift, crucial for identifying the state of chemical bonds. Combining XPS spectra with Fourier-transform

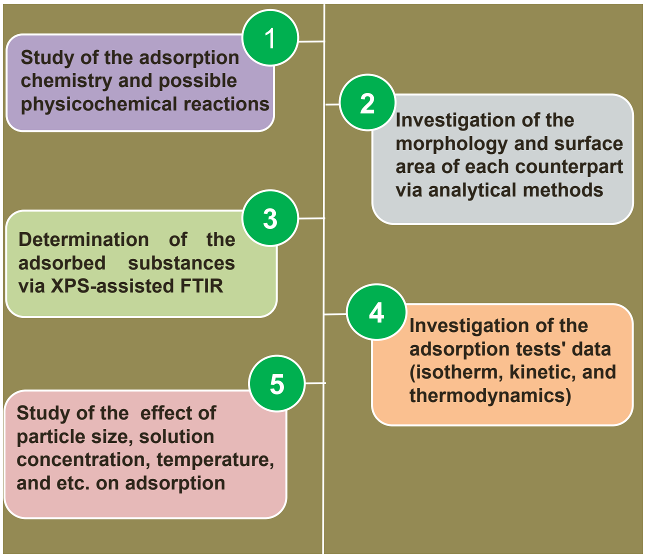

Fig. 7. Main steps to determine the adsorption mechanism.

infrared spectroscopy (FTIR) spectra allows for valuable insights into the adsorption of various substances on the adsorbent surface. The presence and changes in functional groups and the charge of metal ions are key factors in understanding the adsorption mechanism [118]. Kumar et al. investigated the binding between Cu(II) and Cr(VI) ions with a GO/SiO_2@PANI composite using FTIR assisted XPS analysis [79]. By analyzing FTIR peaks of SiO_2 functional groups, they observed a compressed SiO_2 network that was preserved in GO/SiO_2@PANI after fabrication and functionalization. XPS analysis examined the binding of both metal ions onto GO/SiO_2@PANI. Slight changes in the binding

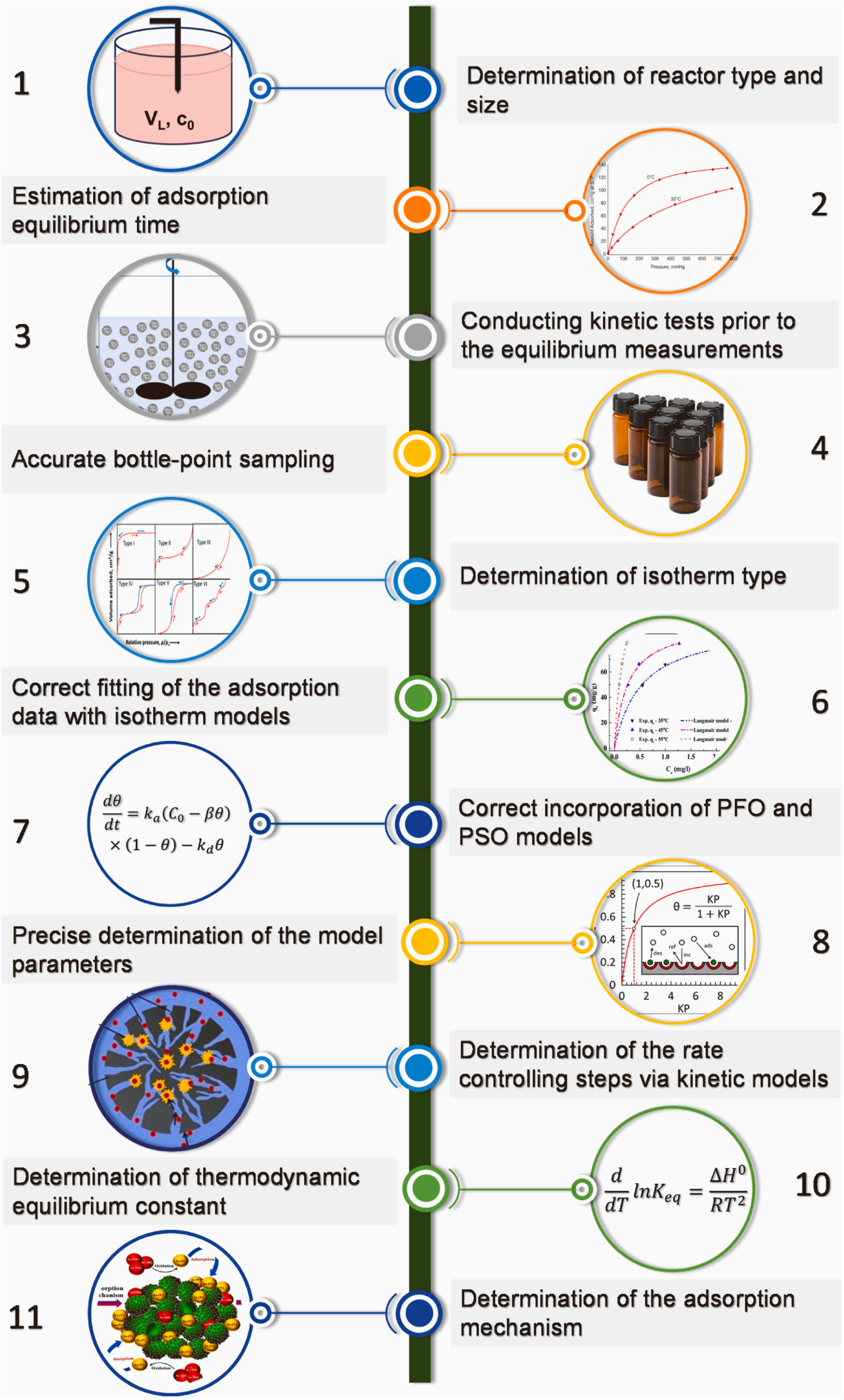

Fig. 8. The main steps in conducting adsorption experiments to evaluate adsorption kinetics, isotherms and thermodynamics in aqueous solutions.

energies and the appearance of new peaks confirmed the interaction between metal ions and the composite. The reduction of Cr(VI) to Cr(III) during adsorption was explained via a multiple-stage mechanism: (i) Optimum removal of Cr(VI) occurs at pH 3, where it adsorbed electrostatically on active sites (-N^+-, -OH_2^+ of GO/SiO_2@PANI). (ii) Electron-rich N-containing functional groups reducing Cr(III) from Cr(VI). (iii) Deprotonated –N- groups of PANI, carboxylic and hydroxyl groups of the GO and SiO_2 adsorbing Cr(III) [79].

The results above demonstrate the potential of simultaneous FTIR-XPS analysis in investigating the adsorption mechanism. With a solid understanding of the chemistry of adsorption, various techniques such as adsorption isotherms, kinetics, and thermodynamics can be employed, along with the examination of factors such as particle size, solution concentration, and temperature, to gain a comprehensive understanding of the adsorption mechanism.

7. Concluding remarks and perspectives

This work assesses equilibrium, kinetics and thermodynamics of PANI-based adsorbents in the removal of pollutants. It attempts to standardize the determination of adsorption equilibrium data, kinetic rates, equilibrium time, and adsorption capacity. To address inaccuracies and miscalculations in conducting adsorption experiments and analyzing results, specific conditions for adsorption experiments and analysis are provided. These conditions can significantly impact the fitting of isotherm and kinetic models and minimize errors in determining thermodynamic parameters. A series of steps (Fig. 8) are recommended for conducting adsorption tests and evaluating the adsorption kinetics, isotherms and thermodynamics in aqueous solutions.

This study also discusses the incorrect use of isotherm models in evaluating thermodynamic parameters and proposes better supported methods. It addresses the erroneous practice of adsorption isotherm constants for calculating thermodynamic parameters in van't Hoff equation, emphasizing the lack of a well-established theoretical relationship between the isotherm constant and thermodynamic equilibrium constant. We also discuss derivation of the Langmuir isotherm model from reaction and equilibrium relations. This reveals the dimensionless Langmuir adsorption coefficient, a vital parameter capturing the essence of adsorption with a theoretically verified approach. Through this approach, the equilibrium constant through the distribution or partition coefficient can be determined. This contributes significantly to the fundamental understanding of adsorption processes and offers a validated framework for determining key thermodynamic parameters.

The comprehensive examination of kinetic models and their features and limitations suggests that it is not reasonable to use the PSO model to determine chemisorption. The application of nonlinear regression methods, diffusion models, and the evaluation of variables, including agitation speed, sorbent diameter, solute concentration, and determination of activation energy, adsorbent mass and operating temperature are recommended to accurately determine the adsorption mechanism. The main steps involved in determining the adsorption mechanism via physiochemical studies and adsorption experiments are outlined. It is concluded that removal of aqueous pollutants by PANI-based adsorbents, characterized by a plethora of nitrogen rich functional amine and imine groups in a well-designed experimental setup, primarily involves monolayer chemisorption, while heterogeneous or homogeneous adsorption may be observed, depending on the morphological nature and distribution of the functional groups.

In future adsorption studies, the methodology in this work can be further refined based on specific conditions, and its application can also be expanded to a broader range of sorbents beyond PANI. In addition, the models involved in the methodology should be tested with the results and data from large-scale studies, and long-term investigations using real wastewater containing contaminants. Maximizing the advantages of adsorption technology and related methodology calls for collaboration between scientists, engineers, and end-users.

CRediT authorship contribution statement

Qingyi Zeng: Writing – review & editing, Visualization, Validation, Methodology, Investigation. **Shuaifei Zhao:** Writing – review & editing, Validation, Supervision, Methodology, Investigation, Conceptualization. **Wenshan Guo:** Writing – review & editing, Validation, Investigation. **Mika Sillanpää:** Writing – review & editing, Validation, Investigation. **Inci Boztepe:** Writing – review & editing, Validation, Methodology. **Chengwen Song:** Writing – review & editing, Validation, Investigation. **Akbar Samadi:** Writing – original draft, Visualization, Validation, Methodology, Investigation, Formal analysis, Data curation, Conceptualization. **Lingxue Kong:** Writing – review & editing, Validation, Supervision, Resources, Methodology, Investigation.

Declaration of Competing Interest

The authors declare that they have no known competing financial interests or personal relationships that could have appeared to influence the work reported in this paper.

Data Availability

Data will be made available on request.

References

[1] Y. Yang, Z. Xiong, Z. Wang, Y. Liu, Z. He, A. Cao, L. Zhou, L. Zhu, S. Zhao, Super-adsorptive and photo-regenerable carbon nanotube based membrane for highly efficient water purification, J. Membr. Sci. 621 (2021) 119000.

[2] M. Jiang, K. Ye, J. Lin, X. Zhang, W. Ye, S. Zhao, B. Van der Bruggen, Effective dye purification using tight ceramic ultrafiltration membrane, J. Membr. Sci. 566 (2018) 151–160.

[3] S. Zhao, L. Zou, C.Y. Tang, D. Mulcahy, Recent developments in forward osmosis: opportunities and challenges, J. Membr. Sci. 396 (2012) 1–21.

[4] Y. You, Y. Ma, Z. Komeily Nia, Y. Su, W. Lei, S. Zhao, J. Li, Adsorption-solubilization controlled extraction of pyrene from surfactant solutions by graphene oxide, J. Environ. Chem. Eng. 12 (2024) 111765.

[5] A. Samadi, M. Xie, J. Li, H. Shon, C. Zheng, S. Zhao, Polyaniline-based adsorbents for aqueous pollutants removal: a review, Chem. Eng. J. (2021) 129425.

[6] A. Samadi, S. Zhao, Polyaniline-based adsorbents and photocatalysts for the elimination of toxic heavy metals, in: Advanced Materials for a Sustainable Environment, CRC Press, 2022, pp. 101–122.

[7] S. Dutta, K. Manna, S.K. Srivastava, A.K. Gupta, M.K. Yadav, Hollow polyaniline microsphere/Fe 3 O 4 nanocomposite as an effective adsorbent for removal of arsenic from water, Sci. Rep. 10 (2020) 1–14.

[8] A. Samadi, Z. Wang, S. Wang, S.K. Nataraj, L. Kong, S. Zhao, Polyaniline-based adsorbents for water treatment: roles of low-cost materials and 2D materials, Chem. Eng. J. 478 (2023) 147506.

[9] M. Duhan, R. Kaur, Phytic acid doped polyaniline nanofibers: an advanced adsorbent for methylene blue dye, Environ. Nanotechnol., Monit. Manag. 12 (2019) 100248.

[10] R. Kaur, M. Duhan, Polyaniline as an inceptive dye adsorbent from effluent, in: Advanced Materials for Wastewater Treatment, John Wiley & Sons, Inc, 2017, pp. 51–99.

[11] D.K. Yoo, N. Abedin Khan, S.H. Jhung, Polyaniline-loaded metal-organic framework MIL-101(Cr): promising adsorbent for CO2 capture with increased capacity and selectivity by polyaniline introduction, J. CO2 Util. 28 (2018) 319–325.

[12] S. Mondal, U. Rana, P. Das, S. Malik, Network of polyaniline nanotubes for wastewater treatment and oil/water separation, ACS Appl. Polym. Mater. 1 (2019) 1624–1633.

[13] O.S. Ekande, M. Kumar, Review on polyaniline as reductive photocatalyst for the construction of the visible light active heterojunction for the generation of reactive oxygen species, J. Environ. Chem. Eng. (2021) 105725.

[14] E.N. Zare, A. Motahari, M. Sillanpää, Nanoadsorbents based on conducting polymer nanocomposites with main focus on polyaniline and its derivatives for removal of heavy metal ions/dyes: a review, Environ. Res. 162 (2018) 173–195.

[15] A. Samadi, A.H. Navarchian, Separation of carbon dioxide from natural gas by matrimid-based mixed matrix membranes, Gas. Process. J. 4 (2016) 1–18.

[16] B. Shi, H. Li, X. Fu, C. Zhao, A.H. Wang, W. Tan, Y. Rao, M. Li, S. Komarneni, H. Yang, Insight into the key role of imine groups in polyaniline for adsorbing heavy metal ions: Density functional theory and experimental study, Sep. Purif. Technol. 335 (2024) 125866.

[17] M. Beygisangchin, S. Abdul Rashid, S. Shafie, A.R. Sadrolhosseini, H.N. Lim, Preparations, properties, and applications of polyaniline and polyaniline thin films-a review, Polymers 13 (2021) 2003.

[18] Kenry, B. Liu, Recent advances in biodegradable conducting polymers and their biomedical applications, Biomacromolecules 19 (2018) 1783–1803.

[19] Y. Xia, T. Li, J. Chen, C. Cai, Polyaniline (skin)/polyamide 6 (core) composite fiber: Preparation, characterization and application as a dye adsorbent, Synth. Met. 175 (2013) 163–169.

[20] A. Bekhoukh, M. Kiari, I. Moulefera, L. Sabantina, A. Benyoucef, New hybrid adsorbents based on polyaniline and polypyrrole with silicon dioxide: synthesis, characterization, kinetics, equilibrium, and thermodynamic studies for the removal of 2,4-dichlorophenol, Polym. (Basel) 15 (2023) 2032.

[21] M.-R. Huang, H.-J. Lu, X.-G. Li, Efficient multicyclic sorption and desorption of lead ions on facilely prepared poly(m-phenylenediamine) particles with extremely strong chemoresistance, J. Colloid Interface Sci. 313 (2007) 72–79.

[22] J. Han, J. Dai, R. Guo, Highly efficient adsorbents of poly(o-phenylenediamine) solid and hollow sub-microspheres towards lead ions: a comparative study, J. Colloid Interface Sci. 356 (2011) 749–756.

[23] X.-G. Li, X.-L. Ma, J. Sun, M.-R. Huang, Powerful reactive sorption of silver (I) and mercury (II) onto poly (o-phenylenediamine) microparticles, Langmuir 25 (2009) 1675–1684.

[24] M.R. Samani, S.M. Borghei, A. Olad, M.J. Chaichi, Removal of chromium from aqueous solution using polyaniline – Poly ethylene glycol composite, J. Hazard. Mater. 184 (2010) 248–254.

[25] M. Bhaumik, A. Maity, V. Srinivasu, M.S. Onyango, Removal of hexavalent chromium from aqueous solution using polypyrrole-polyaniline nanofibers, Chem. Eng. J. 181 (2012) 323–333.

[26] G. Yi, J. Li, L.C. Henderson, W. Lei, L. Du, S. Zhao, Enhancing thermal conductivity of polyvinylidene fluoride composites by carbon fiber: length effect of the filler, Polym. (Basel) 14 (2022) 4599.

[27] W. Huang, S. Wang, D. Li, Polymers and Polymer Composites for Adsorptive Removal of Dyes in Water Treatment, in: Inamuddin, S. Thomas, R. Kumar Mishra, A.M. Asiri (Eds.), Sustainable Polymer Composites and Nanocomposites, Springer International Publishing, Cham, 2019, pp. 519–556.

[28] A. Taghizadeh, M. Taghizadeh, M. Jouyandeh, M.K. Yazdi, P. Zarrintaj, M. R. Saeb, E.C. Lima, V.K. Gupta, Conductive polymers in water treatment: a review, J. Mol. Liq. 312 (2020) 113447.

[29] N. Mennas, S. Lahreche, F. Chouli, L. Sabantina, A. Benyoucef, Adsorption of methylene blue dye by cetyltrimethylammonium bromide intercalated polyaniline-functionalized montmorillonite clay nanocomposite: kinetics, isotherms, and mechanism study, Polym. (Basel) 15 (2023) 3518.

[30] H.-A. Tayebi, Z. Dalirandeh, A. Shokuhi Rad, A. Mirabi, E. Binaeian, Synthesis of polyaniline/Fe3O4 magnetic nanoparticles for removal of reactive red 198 from textile waste water: kinetic, isotherm, and thermodynamic studies, Desalin. Water Treat. 57 (2016) 22551–22563.

[31] Q. Zhou, Y. Wang, J. Xiao, Y. Zhan, Preparation of magnetic core-shell Fe3O4@ polyaniline composite material and its application in adsorption and removal of tetrabromobisphenol A and decabromodiphenyl ether, Ecotoxicol. Environ. Saf. 183 (2019) 109471.

[32] M. Ghorbani, M.S. Lashkenari, H. Eisazadeh, Application of polyaniline nanocomposite coated on rice husk ash for removal of Hg (II) from aqueous media, Synth. Met. 161 (2011) 1430–1433.

[33] D.K.L. Harijan, V. Chandra, Polyaniline functionalized graphene sheets for treatment of toxic hexavalent chromium, J. Environ. Chem. Eng. 4 (2016) 3006–3012.

[34] S. Rastgar, H. Rezaei, H. Yousefi, Study of kinetics, isotherms and thermodynamics of lead adsorption from aqueous solutions using Lignocellulose Nano-fibers (LCNFs), Environ. Resour. Res. 8 (2020) 64–82.

[35] S. Raghav, D. Kumar, Adsorption equilibrium, kinetics, and thermodynamic studies of fluoride adsorbed by tetrametallic oxide adsorbent, J. Chem. Eng. Data 63 (2018) 1682–1697.

[36] S. Azizian, Kinetic models of sorption: a theoretical analysis, J. Colloid Interface Sci. 276 (2004) 47–52.

[37] G.W. Kajjumba, S. Emik, A. Öngen, H.K. Özcan, S. Aydın, Modelling of adsorption kinetic processes—errors, theory and application, in: Advanced Sorption Process Applications, IntechOpen, 2018.

[38] M.A. Al-Ghouti, D.A. Da'ana, Guidelines for the use and interpretation of adsorption isotherm models: a review, J. Hazard. Mater. 393 (2020) 122383.

[39] P.S. Ghosal, A.K. Gupta, Determination of thermodynamic parameters from Langmuir isotherm constant-revisited, J. Mol. Liq. 225 (2017) 137–146.

[40] E.C. Lima, A. Hosseini-Bandegharaei, J.C. Moreno-Piraján, I. Anastopoulos, A critical review of the estimation of the thermodynamic parameters on adsorption equilibria. Wrong use of equilibrium constant in the Van't Hoof equation for calculation of thermodynamic parameters of adsorption, J. Mol. Liq. 273 (2019) 425–434.

[41] Y.-S. Ho, G. McKay, Pseudo-second order model for sorption processes, Process Biochem. 34 (1999) 451–465.

[42] J.-P. Simonin, On the comparison of pseudo-first order and pseudo-second order rate laws in the modeling of adsorption kinetics, Chem. Eng. J. 300 (2016) 254–263.

[43] G.W. Kajjumba, S. Emik, A. Öngen, H.K. Özcan, S. Aydın, Modelling of adsorption kinetic processeses - errors, theory and application. Advanced sorption process applications, IntechOpen, 2018.

[44] S. Debnath, N. Ballav, A. Maity, K. Pillay, Development of a polyaniline-lignocellulose composite for optimal adsorption of Congo red, Int. J. Biol. Macromol. 75 (2015) 199–209.

[45] A. Scott, C. Wild, Transformations and R 2, Am. Stat. 45 (1991) 127–129.

[46] W.J. Weber, J.C. Morris, Kinetics of adsorption on carbon from solution, J. Sanit. Eng. Div. 89 (1963) 31–60.

[47] Y. Liu, L. Song, L. Du, P. Gao, N. Liang, S. Wu, T. Minami, L. Zang, C. Yu, X. Xu, Preparation of polyaniline/emulsion microsphere composite for efficient adsorption of organic dyes, Polym. (Basel) 12 (2020) 167.

[48] S. Sahnoun, M. Boutahala, Adsorption removal of tartrazine by chitosan/polyaniline composite: kinetics and equilibrium studies, Int. J. Biol. Macromol. 114 (2018) 1345–1353.

[49] F. Ishtiaq, H.N. Bhatti, A. Khan, M. Iqbal, A. Kausar, Polypyrole, polyaniline and sodium alginate biocomposites and adsorption-desorption efficiency for imidacloprid insecticide, Int. J. Biol. Macromol. 147 (2020) 217–232.

[50] X. Zhou, X. Zhou, The unit problem in the thermodynamic calculation of adsorption using the Langmuir equation, Chem. Eng. Commun. 201 (2014) 1459–1467.

[51] A. Fenti, P. Iovino, S. Salvestrini, Some remarks on "A critical review of the estimation of the thermodynamic parameters on adsorption equilibria. Wrong use of equilibrium constant in the Van't Hoof equation for calculation of thermodynamic parameters of adsorption", J. Mol. Liq. 273 (2019) 425–434 (2019).

[52] J. Biggar, M. Cheung, Adsorption of picloram (4-amino-3, 5, 6-trichloropicolinic acid) on panoche, ephrata, and palouse soils: a thermodynamic approach to the adsorption mechanism, Soil Sci. Soc. Am. J. 37 (1973) 863–868.

[53] Q. Hu, H. Liu, Z. Zhang, Y. Xie, Nitrate removal from aqueous solution using polyaniline modified activated carbon: optimization and characterization, J. Mol. Liq. (2020) 113057.

[54] Q. Liu, H. Yu, F. Zeng, X. Li, J. Sun, X. Hu, Q. Pan, C. Li, H. Lin, Z. Min Su, Polyaniline as interface layers promoting the in-situ growth of zeolite imidazole skeleton on regenerated cellulose aerogel for efficient removal of tetracycline, J. Colloid Interface Sci. 579 (2020) 119–127.

[55] 5 Adsorption kinetics, in: Adsorption Technology in Water Treatment, De Gruyter, Berlin, Boston, 2012, pp. 123–168..

[56] E. Worch, Adsorption technology in water treatment, in: Adsorption Technology in Water Treatment, de Gruyter, 2021.

[57] G.Z. Kyzas, E.P. Favvas, M. Kostoglou, A.C. Mitropoulos, Effect of agitation on batch adsorption process facilitated by using nanobubbles, Colloids Surf. A Physicochem. Eng. Asp. 607 (2020) 125440.

[58] U.F.C. Sayago, Y.P. Castro, L.R.C. Rivera, A.G. Mariaca, Estimation of equilibrium times and maximum capacity of adsorption of heavy metals by E. crassipes (review), Environ. Monit. Assess. 192 (2020) 141.

[59] Q. Hu, Y. Liu, C. Feng, Z. Zhang, Z. Lei, K. Shimizu, Predicting equilibrium time by adsorption kinetic equations and modifying Langmuir isotherm by fractal-like approach, J. Mol. Liq. 268 (2018) 728–733.

[60] G.J. Millar, S.J. Couperthwaite, C.W. Leung, An examination of isotherm generation: impact of bottle-point method upon potassium ion exchange with strong acid cation resin, Sep. Purif. Technol. 141 (2015) 366–377.

[61] S. Eder, K. Müller, P. Azzari, A. Arcifa, M. Peydayesh, L. Nyström, Mass transfer mechanism and equilibrium modelling of hydroxytyrosol adsorption on olive pit–derived activated carbon, Chem. Eng. J. 404 (2021) 126519.

[62] A. Bonilla-Petriciolet, D.I. Mendoza-Castillo, H.E. Reynel-Ávila, Adsorption Processes for Water Treatment and Purification, Springer, 2017.

[63] J.C. Crittenden, N.J. Hutzler, D.G. Geyer, J.L. Oravitz, G. Friedman, Transport of organic compounds with saturated groundwater flow: model development and parameter sensitivity, Water Resour. Res. 22 (1986) 271–284.

[64] S. Brunauer, Physical adsorption, Adsorpt. gases Vap. 1 (1945) 226.

[65] S.S. Hassan, A.H. Kamel, A.A. Hassan, A.E.-G.E. Amr, A. El-Naby, M.A. Al-Omar, A.Y. Sayed, CuFe2O4/Polyaniline (PANI) Nanocomposite for the hazard mercuric ion removal: synthesis, characterization, and adsorption properties study, Molecules 25 (2020) 2721.

[66] Q. Liu, H. Yu, F. Zeng, X. Li, J. Sun, X. Hu, Q. Pan, C. Li, H. Lin, Z. min Su, Polyaniline as interface layers promoting the in-situ growth of zeolite imidazole skeleton on regenerated cellulose aerogel for efficient removal of tetracycline, J. Colloid Interface Sci. (2020).

[67] Q. Hu, Q. Wang, C. Feng, Z. Zhang, Z. Lei, K. Shimizu, Insights into mathematical characteristics of adsorption models and physical meaning of corresponding parameters, J. Mol. Liq. 254 (2018) 20–25.

[68] M.M. Lakouraj, R.-S. Norouzian, S. Balo, Preparation and Cationic Dye Adsorption of Novel Fe3O4 Supermagnetic/Thiacalix[4]arene Tetrasulfonate Self-Doped/Polyaniline Nanocomposite: Kinetics, Isotherms, and Thermodynamic Study, J. Chem. Eng. Data 60 (2015) 2262–2272.

[69] A. Olad, M. Bastanian, H. Bakht Khosh Hagh, Thermodynamic and kinetic studies of removal process of hexavalent chromium ions from water by using bio-conducting starch–montmorillonite/polyaniline nanocomposite, J. Inorg. Organomet. Polym. Mater. 29 (2019) 1916–1926.

[70] A. Ahmad, H. Ahmad, D. Lokhat, A. Golandaj, D. Ramjugernath, S. Mohd-Setapar, Recent advances in polyaniline-based nanocomposites as potential adsorbents for trace metal ions, in: Polymer-based Nanocomposites for Energy and Environmental Applications, Elsevier, 2018, pp. 597–615.

[71] F.G. Helfferich, Principles of adsorption & adsorption processes, by D. M. Ruthven, John Wiley & Sons, 1984, xxiv + 433 pp, AIChE Journal, 31 (1985) 523-524.

[72] J. Wang, X. Guo, Adsorption kinetic models: Physical meanings, applications, and solving methods, J. Hazard. Mater. 390 (2020) 122156.

[73] D.D. Do, Adsorption Analysis: Equilibria and Kinetics, Imperial College Press, 1998.

[74] A. Khadir, M. Negarestani, H. Ghiasinejad, Low-cost sisal fibers/polypyrrole/polyaniline biosorbent for sequestration of reactive orange 5 from aqueous solutions, J. Environ. Chem. Eng. 8 (2020) 103956.

[75] B. Meroufel, O. Benali, M. Benyahia, Y. Benmoussa, M. Zenasni, Adsorptive removal of anionic dye from aqueous solutions by Algerian kaolin: characteristics, isotherm, kinetic and thermodynamic studies, J. Mater. Environ. Sci. 4 (2013) 482–491 .

[76] A.K. Singh, Chapter 8 - Nanoparticle Ecotoxicology, in: A.K. Singh (Ed.) Engineered Nanoparticles, Academic Press, Boston, 2016, pp. 343-450.

[77] D. Ringot, B. Lerzy, K. Chaplain, J.-P. Bonhoure, E. Auclair, Y. Larondelle, In vitro biosorption of ochratoxin A on the yeast industry by-products: comparison of isotherm models, Bioresour. Technol. 98 (2007) 1812–1821.

[78] F. Akti, M. Okur, The Removal of Acid Violet 90 from Aqueous solutions using pani and pani/clinoptilolite composites: isotherm and kinetics, J. Polym. Environ. 26 (2018) 4233–4242.

[79] R. Kumar, M.A. Barakat, M.A. Taleb, M.K. Seliem, A recyclable multifunctional graphene oxide/SiO2@polyaniline microspheres composite for Cu(II) and Cr(VI) decontamination from wastewater, J. Clean. Prod. 268 (2020) 122290.

[80] W. Lyu, M. Yu, J. Feng, W. Yan, Highly crystalline polyaniline nanofibers coating with low-cost biomass for easy separation and high efficient removal of anionic dye ARG from aqueous solution, Appl. Surf. Sci. 458 (2018) 413–424.

[81] M. Zirpe, H. Bagla, J. Thakur, Rapid Removal of 152+154Eu(III) using polyaniline/ceria nanocomposite from low level waste, J. Inorg. Organomet. Polym. Mater. (2020).

[82] M. Duhan, R. Kaur, Adsorptive removal of methyl orange with polyaniline nanofibers: an unconventional adsorbent for water treatment, Environ. Technol. (2019) 1–14.

[83] F. Berg, J. Wilken, C.A. Helm, S. Block, AFM-based quantification of conformational changes in DNA caused by reactive oxygen species, J. Phys. Chem. B 119 (2015) 25–32.

[84] O. Çelebi, Ç. Üzüm, T. Shahwan, H.N. Erten, A radiotracer study of the adsorption behavior of aqueous Ba2+ ions on nanoparticles of zero-valent iron, J. Hazard. Mater. 148 (2007) 761–767.

[85] M. Tanzifi, S.H. Hosseini, A.D. Kiadehi, M. Olazar, K. Karimipour, R. Rezaiemehr, I. Ali, Artificial neural network optimization for methyl orange adsorption onto polyaniline nano-adsorbent: kinetic, isotherm and thermodynamic studies, J. Mol. Liq. 244 (2017) 189–200.

[86] M. Shabandokht, E. Binaeian, H.-A. Tayebi, Adsorption of food dye Acid red 18 onto polyaniline-modified rice husk composite: isotherm and kinetic analysis, Desalin. Water Treat. (2016) 1–13.

[87] Y. Zheng, W. Wang, D. Huang, A. Wang, Kapok fiber oriented-polyaniline nanofibers for efficient Cr (VI) removal, Chem. Eng. J. 191 (2012) 154–161.

[88] J. Febrianto, A.N. Kosasih, J. Sunarso, Y.-H. Ju, N. Indraswati, S. Ismadji, Equilibrium and kinetic studies in adsorption of heavy metals using biosorbent: a summary of recent studies, J. Hazard. Mater. 162 (2009) 616–645.

[89] M. Mohamed, A. Dolatkhah, T. Aboumourad, L. Dehabadi, L. Wilson, Investigation of templated and supported polyaniline adsorbent materials, RSC Adv. 5 (2015) 6976–6984.

[90] J. Wang, X. Han, Y. Ji, H. Ma, Adsorption of Cr(VI) from aqueous solution onto short-chain polyaniline/palygorskite composites, Desalin. Water Treat. 56 (2014) 356–365.

[91] Y.-d Liang, Y.-j He, Y.-h Zhang, Q.-q zhu, Adsorption property of alizarin red S by NiFe2O4/polyaniline magnetic composite, J. Environ. Chem. Eng. 6 (2018) 416–425.

[92] V. Sharma, P. Rekha, P. Mohanty, Nanoporous hypercrosslinked polyaniline: an efficient adsorbent for the adsorptive removal of cationic and anionic dyes, J. Mol. Liq. 222 (2016) 1091–1100.

[93] S.K. Lagergren, About the theory of so-called adsorption of soluble substances, Sven. Vetensk. Handingarl 24 (1898) 1–39.

[94] E. El-Sharkaway, R.M. Kamel, I.M. El-Sherbiny, S.S. Gharib, Removal of methylene blue from aqueous solutions using polyaniline/graphene oxide or polyaniline/reduced graphene oxide composites, Environ. Technol. (2019) 1–9.

[95] J. Liu, Z. Chen, K. Yu, Y. Liu, Y. Ge, S. Xie, Polyaniline/oxidation etching graphitic carbon nitride composites for U (VI) removal from aqueous solutions, J. Radioanal. Nucl. Chem. 321 (2019) 1005–1017.

[96] X. Liu, B. Wang, G. Jing, Y. Qiao, Kinetics, isotherms, and mechanism of Cr (VI) adsorption by polyaniline/sunflower stem pith composite adsorbent, DESALINATION WATER Treat. 141 (2019) 197–207.

[97] H. Soltani, A. Belmokhtar, F.Z. Zeggai, A. Benyoucef, S. Bousalem, K. Bachari, Copper(II) removal from aqueous solutions by pani-clay hybrid material: fabrication, characterization, adsorption and kinetics study, J. Inorg. Organomet. Polym. Mater. 29 (2019) 841–850.

[98] S. Jadhav, D. Jaspal, Adsorptive eradication of tartrazine from aqueous solutions onto doped polyaniline, 2020, 85 (2020) 13.

[99] S.M. Ahmed, F.I. El-Dib, N.S. El-Gendy, W.M. Sayed, M. El-Khodary, A kinetic study for the removal of anionic sulphonated dye from aqueous solution using nano-polyaniline and Baker's yeast, Arab. J. Chem. 9 (2016) S1721–S1728.

[100] C. Sun, B. Xiong, Y. Pan, H. Cui, Adsorption removal of tannic acid from aqueous solution by polyaniline: Analysis of operating parameters and mechanism, J. Colloid Interface Sci. 487 (2017) 175–181.

[101] M.K.M. Nodeh, S. Soltani, S. Shahabuddin, H.R. Nodeh, H. Sereshti, Equilibrium, kinetic and thermodynamic study of magnetic polyaniline/graphene oxide based nanocomposites for ciprofloxacin removal from water, J. Inorg. Organomet. Polym. Mater. 28 (2018) 1226–1234.

[102] D. Balarak, A.H. Mansouri, K. Chandrika, Adsorption characteristics of metronidazole from industrial wastewater onto polyaniline nanocomposite, Int J. Life Sci. Pharm. Res 9 (2019) 49–58.

[103] D.L. Sparks, Kinetics of Soil Chemical Processes, Academic press, 2013.

[104] R. Gonte, G. Shelar, K. Balasubramanian, Polymer–agro-waste composites for removal of Congo red dye from wastewater: adsorption isotherms and kinetics. (in), Desalin. Water Treat. 52 (2014) 7797–7811 (in).

[105] M. Sarkar, P.K. Acharya, B. Bhattacharya, Modeling the adsorption kinetics of some priority organic pollutants in water from diffusion and activation energy parameters, J. Colloid Interface Sci. 266 (2003) 28–32.

[106] H. Javadian, Application of kinetic, isotherm and thermodynamic models for the adsorption of Co(II) ions on polyaniline/polypyrrole copolymer nanofibers from aqueous solution, J. Ind. Eng. Chem. 20 (2014) 4233–4241.

[107] R. Ahmad, I. Hasan, A. Mittal, Adsorption of Cr (VI) and Cd (II) on chitosan grafted polyaniline-OMMT nanocomposite: isotherms, kinetics and thermodynamics studies, Desalin. Water Treat. 58 (2017) 144–153.

[108] F.-C. Wu, R.-L. Tseng, R.-S. Juang, Characteristics of Elovich equation used for the analysis of adsorption kinetics in dye-chitosan systems, Chem. Eng. J. 150 (2009) 366–373.

[109] R. Ahmad, Polyaniline/ZnO nanocomposite: a novel adsorbent for the removal of Cr (VI) from aqueous solution, in: Advances in Composite Materials Development, IntechOpen, 2019.

[110] X. Geng, T. Han, C. Cao, Adsorption enthalpy and desorption enthalpy during displacement of adsorbate to solvent in a liquid-solid system, J. Therm. Anal. Calorim. 45 (1995) 157–165.

[111] R. Chang, Physical Chemistry for the Chemical and Biological Sciences, University Science Books, 2000.

[112] F.-D. Kopinke, A. Georgi, K.-U. Goss, Comment on "Mistakes and inconsistencies regarding adsorption of contaminants from aqueous solution: a critical review, published by Tran et al.[Water Research 120, 2017, 88–116]", Water Res. 129 (2018) 520–521.

[113] E.C. Lima, A. Hosseini-Bandegharaei, I. Anastopoulos, Response to "Some remarks on a critical review of the estimation of the thermodynamic parameters on adsorption equilibria. Wrong use of equilibrium constant in the van't Hoff equation for calculation of thermodynamic parameters of adsorption, J. Mol. Liq. 273 (2019) 425–434. Journal of Molecular Liquids, 280 (2019) 298-300.

[114] H.N. Tran, S.-J. You, A. Hosseini-Bandegharaei, H.-P. Chao, Mistakes and inconsistencies regarding adsorption of contaminants from aqueous solutions: a critical review, Water Res. 120 (2017) 88–116.

[115] H. Lei, N. Pan, X. Wang, H. Zou, Facile synthesis of phytic acid impregnated polyaniline for enhanced U(VI) adsorption, J. Chem. Eng. Data 63 (2018) 3989–3997.

[116] Y. Fu, R.S. Hansen, F. Bartell, Thermodynamics of Adsorption from Solutions. I. The Molality and Activity" co-efficient of adsorbed layers, J. Phys. Chem. 52 (1948) 374–386.

[117] S. Ray, A.G. Shard, Quantitative analysis of adsorbed proteins by X-ray photoelectron spectroscopy, Anal. Chem. 83 (2011) 8659–8666.

[118] B. Gao, Y. Li, Z. Chen, Adsorption behaviour of functional grafting particles based on polyethyleneimine for chromate anions, Chem. Eng. J. 150 (2009) 337–343.